Analysis of luminescence decay dynamics in metal-dielectric photonic structures with organic layers

© K.M. Morozov[1], A.V. Belonovskii[1], M.A. Kaliteevski[2]

[1] Alferov Federal State Budgetary Institution of Higher Education and Science Saint Petersburg National Research Academic University of the Russian Academy of Sciences, 194021 St. Petersburg, Russia
[2] ITMO University, 197101 St. Petersburg, Russia

E-mail: morzconst@gmail.com

Received November 4, 2022
Revised November 29, 2022
Accepted November 30, 2022

Metal-dielectric photonic structures with organic materials 4,4-bis(N-carbazolyl)-1,1-biphenyl and 4,4′-bis[4-(di-ptolylamino)styryl]biphenyl) as light emitting layers were investigated. The formation of the polaritonic modes in the investigated structures was experimentally demonstrated and a correlation between theoretical and experimental dispersion was shown. Was shown, that increase in interaction between organic exciton and optical mode leads to a significant decrease in the lower polariton emission bandwidth.

Keywords: light-emitting layers, exciton, luminescence.

DOI: 10.21883/SC.2022.12.55149.4291

1. Introduction

The study of photonic nanostructures has presently become one of the most rapidly advancing and promising fields of applied science. The use of photonic nanostructures, which allow one to localize and control the propagation of light within them, becomes a common practice for enhancing the efficiency of existing optoelectronic systems and a basis for potential device applications. Photonic structures with metallic elements (plasmonic structures) have also attracted considerable research attention in recent years [1]. The structure with a Tamm plasmon [2,3] is an often-studied type of metal–dielectric structures. This microcavity design is widely used for various types of materials of the active region (e.g., semiconductor quantum dots [4]), since it offers relative ease of fabrication (while maintaining high Q factors of the optical mode) and provides ample opportunities for control over the cavity parameters via adjustment of the geometric structure parameters.

Organic semiconductor materials offer a number of features that were used to construct flexible and environmentally friendly new-generation LEDs [5,6]. A series of organic small molecules and polymers with different optical properties and a very wide range of emission energies have already been synthesized [7]. However, organic materials pumped by an electric current produce more triplet excited states than singlet ones (the ratio is 1 : 3). Since radiative relaxation of triplets to the ground state is forbidden in the dipole approximation, the efficiency of such systems is limited to 25%. However, certain approaches to stimulation of triplet relaxation, which maximize the efficiency, have been proposed. Among them is the use of rare-earth metals [8] and systems supporting thermally activated delayed fluorescence [9]. The interaction with a localized optical mode may also modify significantly the processes of relaxation of emitters [10]. Microcavities operating in the strong coupling regime have been used in recent studies [11–13] to split the singlet level of an organic molecule, reduce the energy detuning between the triplet and the lower polariton mode, and, consequently, intensify the process of delayed fluorescence.

Thus, the study of characteristics of organic microcavities and the influence of interactions with the optical cavity mode on relaxation processes is important for potential applications in organic light-emitting devices with an enhanced efficiency. Metal–dielectric cavities with a Tamm plasmon, which are formed by a dielectric layered mirror and a thin metallic mirror, are a convenient and promising platform for fabrication and examination of organic materials interacting with light. In the present study, we report the results of examination of properties of metal–dielectric cavity structures with organic light-emitting CBP (4,4-bis(N-carbazolyl)-1,1-biphenyl) and DPAVBi (4,4′-bis [4-(di-ptolylamino)styryl]biphenyl) layers.

2. Design and fabrication of samples and measurement procedure

Structures with a Tamm plasmon were fabricated using several processing techniques. At the first stage, specialized Bragg reflectors based on SiO_2/Ta_2O_5 were formed by magnetron deposition. Layers of organic materials and metals were deposited successively onto prepared substrates using a Kurt. J. Lesker Spectros thin-film vacuum (up to 10^{-5} mbar) thermal deposition system. Organic materials

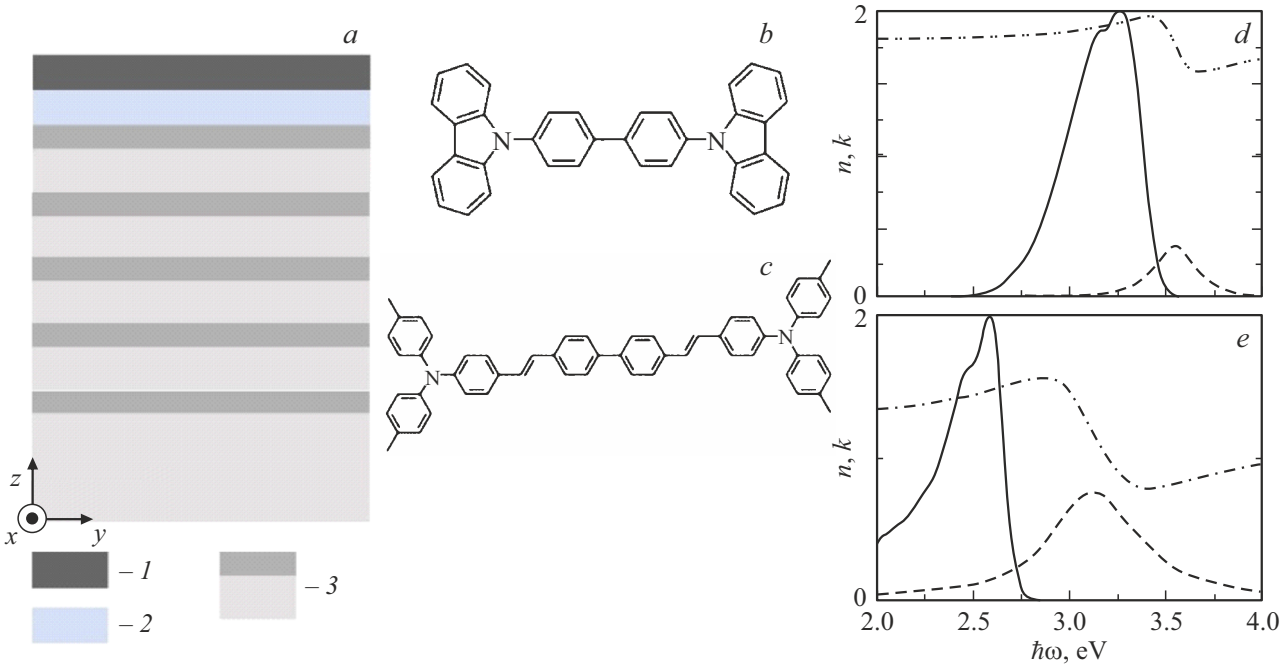

Figure 1. (*a*) Design of the metal–dielectric microcavity structure with an organic light-emitting layer: *1* — metallic mirror, *2* — organic material layer, *3* — period of the distributed Bragg reflector. (*b, c*) Molecular structure and (*d, e*) optical properties of organic CBP and DPAVBi materials.

(CBP, DPAVBi) were deposited at a rate of 0.1 nm/s. A thin silver layer was deposited at a rate of ~ 0.05 nm/s with a source temperature of $\sim 962^\circ$C. Reference layers of CBP, DPAVBi, and silver were deposited onto the SiO_2 substrate (alongside with the process of deposition onto the Bragg mirror) to control the thickness of organic layers and measure photoluminescence (PL) spectra of materials outside of the microcavity. The thickness of deposited reference layers was measured with a JA Woollam VASE ellipsometer. The fabricated samples were examined using an ellipsometer that had the capacity to measure angle-resolved reflection spectra (within the range from 20 to 90°). Room-temperature PL spectra were also measured under 45-degree incidence of light with a Jobin-Yvon Horiba Fluorolog FL3-22 spectrometer, which uses a 450 W xenon lamp with a monochromator as a light source. The obtained reflection spectra were approximated with the Lorentz function to determine the position of features (dips in the spectrum).

The typical design of a metal–dielectric microcavity with an organic light-emitting layer is presented in Fig. 1, *a*. The studied structure with a Tamm plasmon consists of a thin metal layer, a Bragg reflector, and an organic material layer sandwiched between them. The engineering of a metal–dielectric microcavity (determination of the needed thicknesses of component layers) starts with examining the optical properties of organic materials: the refraction index spectrum and the emission spectrum. The molecular structure of organic materials CBP (4,4-bis(N-carbazolyl)-1,1-biphenyl) and DPAVBi (4,4′-bis[4-(di-ptolylamino)styryl]biphenyl), which are considered in the present study, is presented in Figs. 1, *b* and *c*, respectively. Figures 1, *d, e* show the emission (solid curve) and refraction index (dashed curve — imaginary part; dash-and-dot curve — real part) spectra of CBP and DPAVBi.

Parameters defining the refraction indices of organic materials

Material	ϵ_b	$\hbar\omega_{\text{exc}}$, eV	$\hbar\omega_{LT}$, eV	$\hbar\omega_{\text{exc}}$, meV
CBP	3.9	3.5	0.026	150
DPAVBi	3.02	3.05	1.02	240

The studied organic materials feature a wide luminescence band (~ 420 meV for CBP and 330 meV for DPAVBi). The presented refraction index is an approximation of the experimentally measured values with the following formula for permittivity:

$$\epsilon(\omega) = \epsilon_b + \frac{\omega_{LT}}{\omega_{\text{exc}} - \omega - i\gamma_{\text{exc}}}, \qquad (1)$$

where ϵ_b is the background permittivity, ω_{exc} is the exciton frequency, ω_{LT} is the longitudinal-transverse splitting parameter proportional to the oscillator strength, and γ_{exc} is nonradiative decay. The parameters used are listed in the table. The spectral dependence for the imaginary part of the CBP refraction index features a peak corresponding to the exciton resonance with an energy of 3.5 eV. A strong exciton resonance may interact efficiently with the microcavity mode and induce splitting into two polariton modes (interaction in the strong coupling regime). The energies of

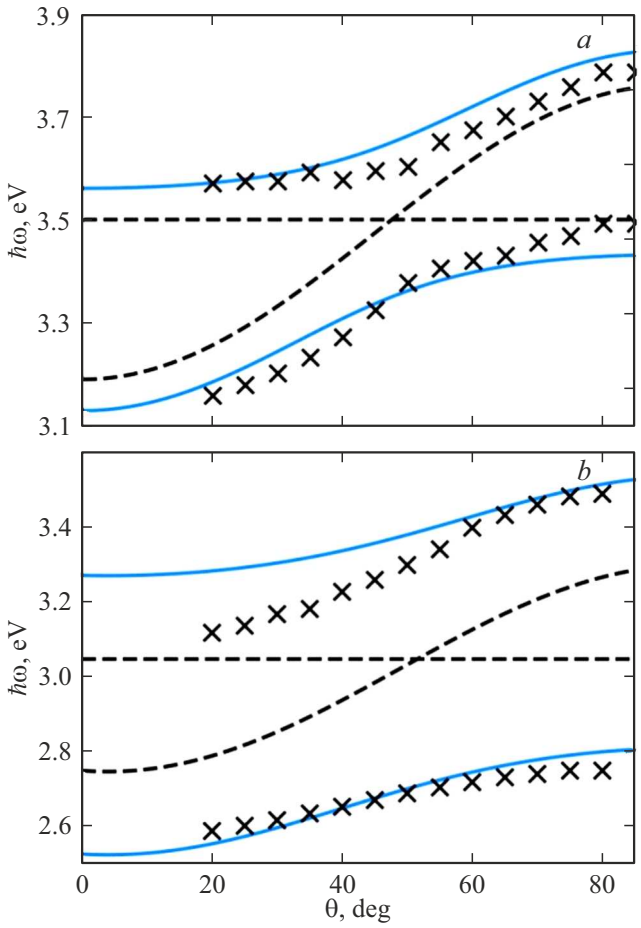

Figure 2. Angular dispersion of polariton modes for the structures with CBP (a) and DPAVBi (b). Crosses denote the positions of polariton modes determined experimentally, while solid curves are the mode dispersions obtained using expression (2). Dashed curves represent the exciton energy in the organic material and the Tamm plasmon mode dispersion.

an exciton and the optical cavity mode need to be close for the strong coupling regime to be established.

The following thicknesses of Bragg reflector layers were chosen in fabrication of the cavity: Bragg reflectors for CBP and DPAVBi have five pairs of SiO_2/Ta_2O_5 layers with a thickness of 66 and 75 nm (SiO_2) and 43 and 49 nm (Ta_2O_5), respectively. The CBP layer thickness was 26 nm, and the thickness of DPAVBi was 40 nm. A thin (50 nm) silver layer was used as a top metallic mirror in cavities with both organic materials. The above parameters for the structure with CBP provided the optimum mode energy under normal incidence (3.19 eV) for establishing the strong coupling regime (see Fig. 2, a). The mode energy increases with incidence angle and becomes equal to the exciton energy at an angle of $\sim 47°$. Likewise, the mode energy for the structure with DPAVBi under normal incidence is 2.75 eV (differs by 300 meV from the exciton energy) and becomes equal to the exciton energy at an angle of $\sim 51°$ (see Fig. 2, b).

3. Results and discussion

Let us pass on to the theoretical and experimental results. Polariton modes manifest themselves as dips with anticrossing angular dispersion in the reflection spectrum. Angle-resolved reflection spectra of the fabricated structures were measured, and the obtained data were approximated with the Lorentz function. The results of approximation (crosses) for the TE polarization are shown in Figs. 2, a (CBP) and 2, b (DPAVBi). The anticrossing behavior of dispersion of the upper polariton branches is evident. This behavior may be characterized theoretically using the method of coupled oscillators

$$\omega_{UP,LP} = \frac{\omega_{\text{exc}} + \omega_{TP}}{2} - \frac{i(\gamma_{\text{exc}} + \gamma_{TP})}{2} \pm \frac{\Omega}{2}, \qquad (2)$$

where ω_{TP} is the frequency of the metal–dielectric cavity mode, γ_{TP} is its nonradiative decay, and Ω is the splitting energy (Rabi energy). Using the above parameters of organic materials and parameters characterizing the optical mode localized in the structure (ω_{TP}, γ_{TP}), we plotted the

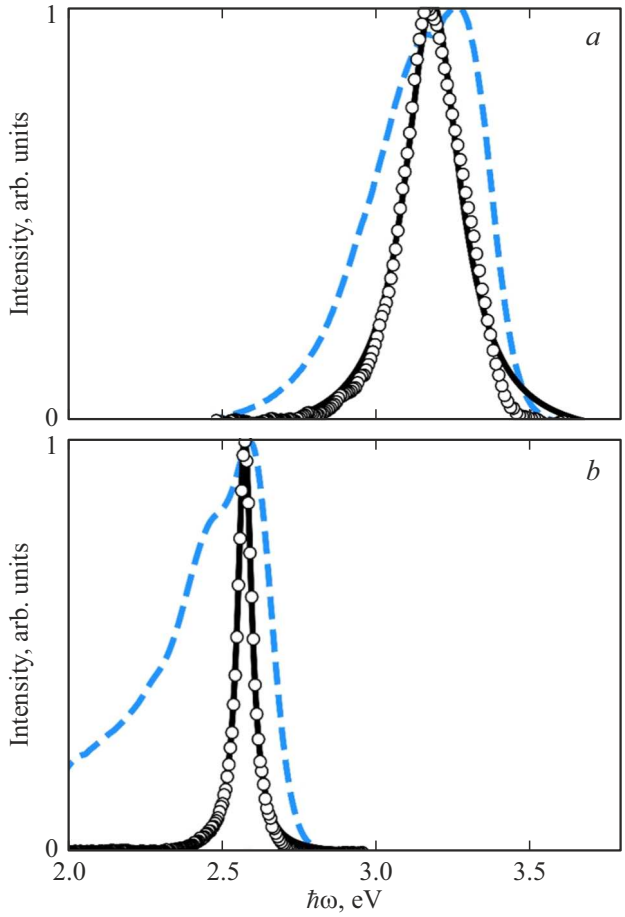

Figure 3. Luminescence spectra of structures with CBP (a) and DPAVBi (b). Dashed curves represent the free-space emission spectra of materials. Circles are the results of measurement of PL spectra of metal–dielectric structures, and solid curves are the Lorentz approximations of luminescence peaks.

dispersions of polariton branches. It turned out that their behavior correlates with the results of experiments.

One may notice that the theoretical and experimental data for the upper polariton branch of the structure with DPAVBi diverge at angles $< 60°$. This may be attributed to the fact that the method of coupled oscillators provides first-approximation estimates of the dispersion of polariton modes, while an allowance for the reduction of the coefficient of reflection from the metallic mirror in this spectral region and the proximity of the edge state of the Bragg reflector should be made in accurate calculations for metal–dielectric structures. The magnitude of Rabi splitting at the anticrossing point for the structures with CPB and DPAVBi is ~ 300 and ~ 676 meV, respectively. It is common practice to distinguish a separate interaction regime (ultrastrong coupling) [14] at the point when the Rabi splitting value becomes comparable ($\sim 20\%$) to the exciton energy.

The luminescence spectra of the fabricated structures were also measured. They are presented in Figs. 3, *a* (CBP) and 3, *b* (DPAVBi). Circles represent the emission spectrum of structures under normal incidence, and solid curves are the Lorentz approximations of the spectrum. It can be seen that the microcavity emission structure differs considerably from the emission of organic materials outside the cavity: the peak is shifted to the region corresponding to the lower polariton branch and is significantly narrower (210 meV for the structure with CBP and 55 meV for DPAVBi). A two-fold reduction in the emission band width for the structure with CBP (and an almost six-fold reduction in the case of DPAVBi) is typical of the strong coupling regime [15]. The width of the emission band from the lower polariton branch decreases as the intensity of interaction between the optical mode and an exciton in an organic material increases.

4. Conclusion

The results of examination of properties of metal–dielectric cavity structures with organic light-emitting CBP (4,4-bis(N-carbazolyl)-1,1-biphenyl) and DPAVBi (4,4′-bis[4-(di-ptolylamino)styryl]biphenyl) layers were reported above. The dispersion of polariton modes was studied theoretically (using the method of coupled oscillators) and experimentally (by measuring angle-resolved reflection spectra with subsequent approximation). The results of modeling agree qualitatively with experimental data. PL spectra under normal incidence were also measured for the fabricated structures. The obtained results demonstrated that a stronger light–matter interaction manifests itself in a greater reduction in the luminescence band width.

Funding

This study was supported by the Ministry of Science and Higher Education of the Russian Federation, project 0791-2020-0002.

Conflict of interest

The authors declare that they have no conflict of interest.

References

[1] M.S. Tame, K.R. McEnery, Ş.K. Özdemir, J. Lee, S.A. Maier, M.S. Kim. Nature Phys., **9**, 329 (2013).
[2] C. Symonds, G. Lheureux, J.P. Hugonin, J.J. Greffet, J. Laverdant, G. Brucoli, A. Lemaitre, P. Senellart, J. Bellessa. Nano Lett., **13**, 3179 (2013).
[3] M.A. Kaliteevski, A.A. Lazarenko, N.D. Il'inskaya, Yu.M. Zadiranov, M.E. Sasin, D. Zaitsev, V.A. Mazlin, P.N. Brunkov, S.I. Pavlov, A.Yu. Egorov. Plasmonics, **10**, 281 (2014).
[4] A.R. Gubaydullin, C. Symonds, J. Bellessa, K.A. Ivanov, E.D. Kolykhalova, M.E. Sasin, A. Lemaitre, P. Senellart, G. Pozina, M.A. Kaliteevski. Sci. Rep., **7**, 9014 (2017).
[5] A. Salehi, X. Fu, D. Shin, F. So. Adv. Funct. Mater., **29**, 1808803 (2019).
[6] D. Luo, Q. Chen, B. Liu, Y. Qiu. Polymers, **11**, 384 (2019).
[7] Q. Wei, N. Fei, A. Islam, T. Lei, L. Hong, R. Peng, X. Fan, L. Chen, P. Gao, Z. Ge. Adv. Opt. Mater., **6**, 1800512 (2018).
[8] H. Yersin, A.F. Rausch, R. Czerwieniec, T. Hofbeck, T. Fischer. Coord. Chem. Rev., **255**, 2622 (2011).
[9] F.B. Dias, J. Santos, D.R. Graves, P. Data, R.S. Nobuyasu, M.A. Fox, A.S. Batsanov, T. Palmeira, M.N. Berberan-Santos, M.R. Bryce, A.P. Monkman. Adv. Sci., **3**, 1600080 (2016).
[10] R.F. Ribeiro, L.A. Martínez-Martínez, M. Du, J. Campos-Gonzalez-Angulo, J. Yuen-Zhou. Chem. Sci., **9**, 6325 (2018).
[11] Y. Yu, S. Mallick, M. Wang, K. Börjesson. Nature Commun., **12**, 3255 (2021).
[12] L.A. Martínez-Martínez, E. Eizner, S. Kéna-Cohen, J. Yuen-Zhou. J. Chem. Phys., **151**, 054106 (2019).
[13] D. Polak, R. Jayaprakash, T.P. Lyons, L.Á. Martínez-Martínez, A. Leventis, K.J. Fallon, H. Coulthard, D.G. Bossanyi, K. Georgiou, II.A.J. Petty, J. Anthony, H. Bronstein, J. Yuen-Zhou, A.I. Tartakovskii, J. Clark, A.J. Musser. Chem. Sci., **11**, 343 (2020).
[14] A. Genco, A. Ridolfo, S. Savasta, S. Patané, G. Gigli, M. Mazzeo. Adv. Opt. Mater., **6**, 1800364 (2018).
[15] P. Schouwink, J.M. Lupton, H. von Berlepsch, L. Dähne, R.F. Mahrt. Phys. Rev. B, **66**, 081203(R) (2002).